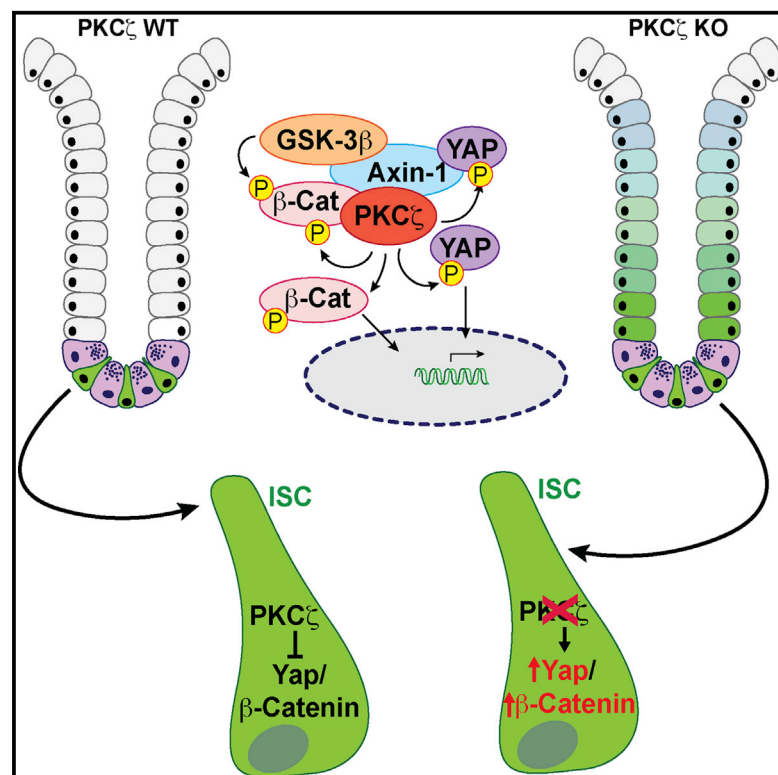


## Repression of Intestinal Stem Cell Function and Tumorigenesis through Direct Phosphorylation of $\beta$ -Catenin and Yap by PKC $\zeta$

### Graphical Abstract



### Authors

Victoria Llado, Yuki Nakanishi, ...,  
Maria T. Diaz-Meco, Jorge Moscat

### Correspondence

jmoscat@sanfordburnham.org

### In Brief

Llado et al. demonstrate that the tumor suppressor PKC $\zeta$  is expressed in Lgr5<sup>+</sup> intestinal stem cells and represses their stemness by inhibiting  $\beta$ -catenin and Yap levels and function through direct phosphorylation. This results in increased intestinal regeneration and tumorigenesis in mice with targeted ablation of PKC $\zeta$  in LGR5<sup>+</sup> cells.

### Highlights

- PKC $\zeta$  is expressed in Lgr5<sup>+</sup> intestinal stem cells
- Loss of PKC $\zeta$  results in increased intestinal stem cell activity
- PKC $\zeta$  deficiency in intestinal stem cells drives regeneration and tumorigenesis
- PKC $\zeta$  reduces  $\beta$ -catenin and Yap levels and function by direct phosphorylation



# Repression of Intestinal Stem Cell Function and Tumorigenesis through Direct Phosphorylation of $\beta$ -Catenin and Yap by PKC $\zeta$

Victoria Llado,<sup>1,5</sup> Yuki Nakanishi,<sup>1,5</sup> Angeles Duran,<sup>1</sup> Miguel Reina-Campos,<sup>1</sup> Phillip M. Shelton,<sup>1</sup> Juan F. Linares,<sup>1</sup> Tomoko Yajima,<sup>1</sup> Alex Campos,<sup>2</sup> Pedro Aza-Blanc,<sup>3</sup> Michael Leitges,<sup>4</sup> Maria T. Diaz-Meco,<sup>1</sup> and Jorge Moscat<sup>1,\*</sup>

<sup>1</sup>Cell Death and Survival Networks Program, Sanford-Burnham Medical Research Institute, 10901 North. Torrey Pines Road, La Jolla, CA 92037, USA

<sup>2</sup>Proteomics Facility, Sanford-Burnham Medical Research Institute, 10901 North. Torrey Pines Road, La Jolla, CA 92037, USA

<sup>3</sup>Functional Genomics Core, Sanford-Burnham Medical Research Institute, 10901 North. Torrey Pines Road, La Jolla, CA 92037, USA

<sup>4</sup>Biotechnology Centre of Oslo, University of Oslo, 0316 Oslo, Norway

<sup>5</sup>Co-first author

\*Correspondence: [jmoscat@sanfordburnham.org](mailto:jmoscat@sanfordburnham.org)

<http://dx.doi.org/10.1016/j.celrep.2015.01.007>

This is an open access article under the CC BY-NC-ND license (<http://creativecommons.org/licenses/by-nc-nd/3.0/>).

## SUMMARY

Intestinal epithelial homeostasis requires continuous renewal supported by stem cells located in the base of the crypt. Disruption of this balance results in failure to regenerate and initiates tumorigenesis. The  $\beta$ -catenin and Yap pathways in Lgr5<sup>+</sup> stem cells have been shown to be central to this process. However, the precise mechanisms by which these signaling molecules are regulated in the stem cell population are not totally understood. Protein kinase C  $\zeta$  (PKC $\zeta$ ) has been previously demonstrated to be a negative regulator of intestinal tumorigenesis. Here, we show that PKC $\zeta$  suppresses intestinal stem cell function by promoting the downregulation of  $\beta$ -catenin and Yap through direct phosphorylation. PKC $\zeta$  deficiency results in increased stem cell activity in organoid cultures and in vivo, accounting for the increased tumorigenic and regenerative activity response of Lgr5<sup>+</sup>-specific PKC $\zeta$ -deficient mice. This demonstrates that PKC $\zeta$  is central to the control of stem cells in intestinal cancer and homeostasis.

## INTRODUCTION

The intestinal epithelium displays a high renewal potential due in large part to the activity of intestinal stem cells (ISCs) (Clevers, 2013). Targeting of the Lgr5 marker gene has recently led to the identification of a type of stem cell located in the mouse small intestine at the bottom of the crypt (Barker et al., 2007, 2009). They give rise to the transit-amplifying (TA) crypt compartment, in which TA cells divide and migrate upward toward the crypt-villus junction (Clevers, 2013). When committed TA cells reach this junction, they rapidly differentiate while continuing their upward migration (Clevers, 2013). This

stem cell population has been shown to be very sensitive to transformation by adenomatous polyposis coli (APC) mutations that rapidly lead to adenoma formation (Barker et al., 2009). In contrast, TA cells, and more differentiated cells within the villus, although also capable of adenoma formation, will only do so after long latency periods (Schwitalla et al., 2013). This suggests that stem cells are the most common origin of intestinal cancer (Barker et al., 2009). Furthermore, Lgr5-expressing cells have been detected within experimental adenomas, and their function has been shown by lineage-tracing assays. This supports the idea that normal tissue stem cells can contribute to cancer initiation and progression and is consistent with the cancer stem cell theory (Schepers et al., 2012). If ISCs are the target of tumor-initiation factors, we can predict that increasing the number or proliferative activity of these cells will increase the risk of intestinal neoplasms as well as hamper their treatment. Therefore, a better understanding of the signaling cascades that regulate stem cell signaling is essential for the design of new and more efficacious therapies for intestinal tumors, as well as tissue regeneration after injury.

We have addressed this fundamental biological problem in the context of protein kinase C  $\zeta$  (PKC $\zeta$ ) deficiency. PKC $\zeta$  and PKC $\lambda/1$  constitute the atypical protein kinase C (aPKC) family. Both aPKCs have been implicated in oncogenic transformation (Moscat et al., 2009). A number of studies support the clinical relevance of PKC $\zeta$  as a tumor suppressor in several tissues, including the intestine (Galvez et al., 2009; Ma et al., 2013). Thus, our own studies demonstrated that PKC $\zeta$  is downregulated in human colorectal cancers as compared to normal colon tissue and is underexpressed in cancers progressing to metastasis (Ma et al., 2013). Interestingly, an inactivation mutation in PKC $\zeta$  (S514F) has been identified in human colon cancers (Galvez et al., 2009; Wood et al., 2007). Our most recent studies demonstrated that PKC $\zeta$  deficiency promotes the plasticity necessary for intestinal cancer cells to reprogram their metabolism in order to survive in the absence of glucose and that the total-body loss of PKC $\zeta$  in mice results in enhanced intestinal tumorigenesis. Those

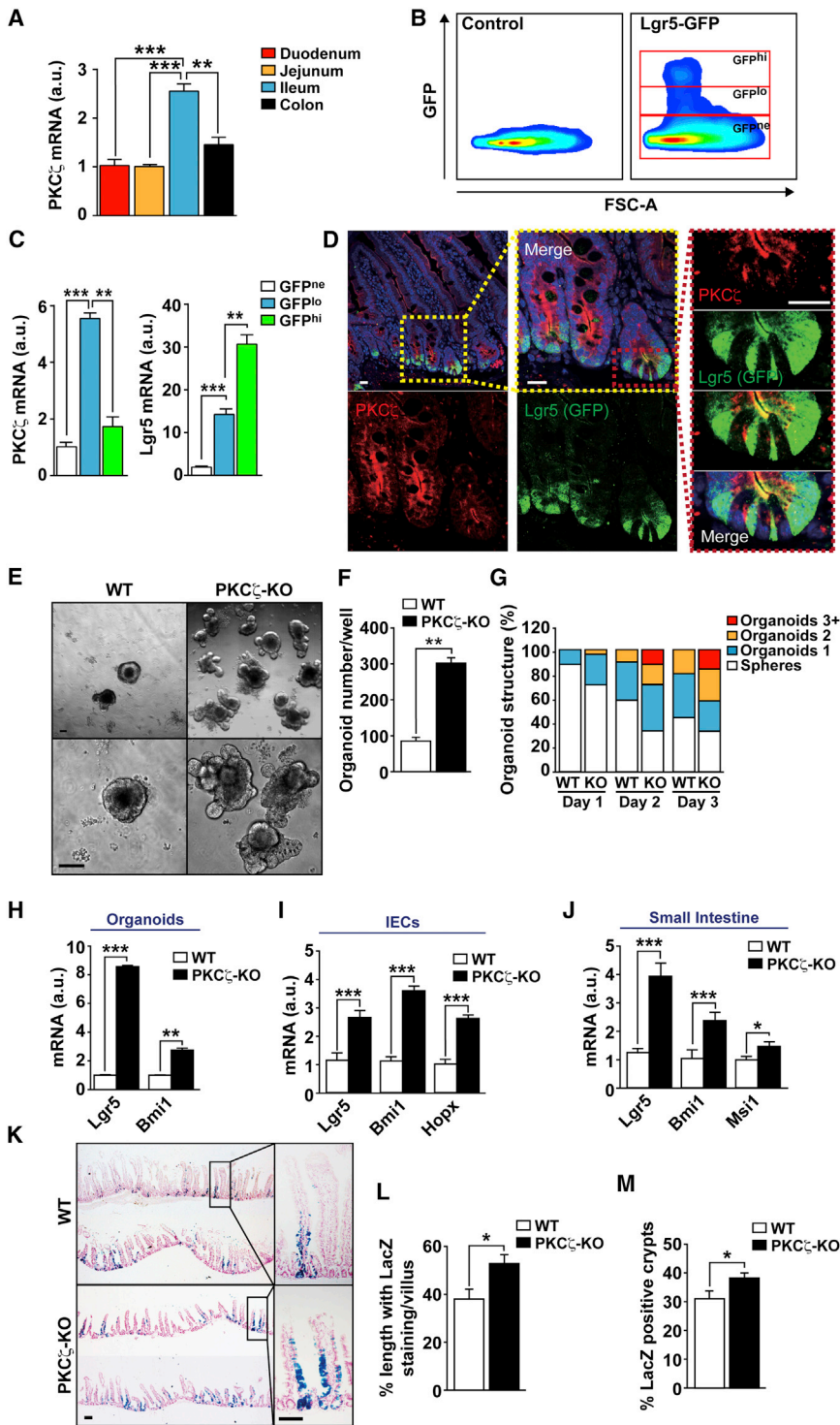


**Figure 1. PKC $\zeta$  Represses Intestinal Stem Cell Activity**

(A) PKC $\zeta$  mRNA levels in intestinal epithelial cells from different intestinal regions (n = 4). (B) Lgr5-GFP<sup>+</sup> cells sorting from control and Lgr5-EGFP-ires-CreERT2 intestine. (C) PKC $\zeta$  and Lgr5 mRNA levels in the different sorted populations (n = 4). (D) Confocal immunofluorescence of PKC $\zeta$  and GFP in Lgr5-EGFP-ires-CreERT2 intestinal sections. Scale bars represent 25  $\mu$ m. (E) Intestinal crypt organoids from WT and PKC $\zeta$  KO mice after 3 days in culture. (F and G) Quantification of number of organoids (F) and organoid structural complexity (G) of experiment shown in (E); n = 6. (H–J) Quantitative analysis of ISC markers in organoids (n = 3) (H), intestinal epithelial cells (n = 6) (I), and small intestine from WT and PKC $\zeta$  KO mice (n = 6) (J). (K) LacZ stained sections of small intestine from Lgr5-WT and Lgr5-PKC $\zeta$  KO mice 5 days after tamoxifen injection. (L and M) Quantification of LacZ-stained cells in the crypt-villus unit (L) and number of blue-labeled intestinal crypts (M). Counting of at least 20 fields of view per mouse (n = 3 mice). Scale bars represent 100  $\mu$ m. Results are presented as mean  $\pm$  SEM. \*p < 0.05, \*\*p < 0.01, \*\*\*p < 0.001. See also Figure S1.

## RESULTS

### Loss of PKC $\zeta$ Results in Increased Intestinal Stem Cell Activity

As a first step in exploring the role of PKC $\zeta$  in ISCs, we used the Lgr5-EGFP-ires-CreERT2 knockin allele mouse strain crossed with Rosa26-LacZ reporter mice to generate Lgr5Cre-Rosa26-LacZ mice. In this mouse model, Lgr5<sup>+</sup> cells were GFP labeled and the Lgr5Cre reporter was activated by the injection of tamoxifen. This strategy allows for the purification of Lgr5<sup>+</sup> cells by sorting using GFP as the marker, as well as the in vivo tracking of the subsequent fate of the progeny of these cells by X-gal staining of intestinal tissue (Barker et al., 2007, 2009). Of note, we found that PKC $\zeta$  was expressed both in the small intestine and in the colon and that its levels were specially enriched in ileum as compared to duodenum or jejunum (Figure 1A). To determine its

results unveiled a critical role for PKC $\zeta$  as a tumor suppressor in cells metabolically stressed during tumor progression (Ma et al., 2013). However, it remains to be determined whether PKC $\zeta$  is important in stem cell function related to tumorigenesis and under noncancer conditions, such as during tissue regeneration.

expression in ISCs, we sorted GFP-positive epithelial cells from crypts isolated from ileum of Lgr5-EGFP-ires-CreERT2 mice. Fluorescence-activated cell sorting analysis distinguished an LGR5-GFP-high (GFP<sup>hi</sup>) cell population, corresponding to the active stem cell pool, and an LGR5-GFP-low (GFP<sup>lo</sup>) fraction that contains the immediate/early non-stem cell progeny (Figure 1B).

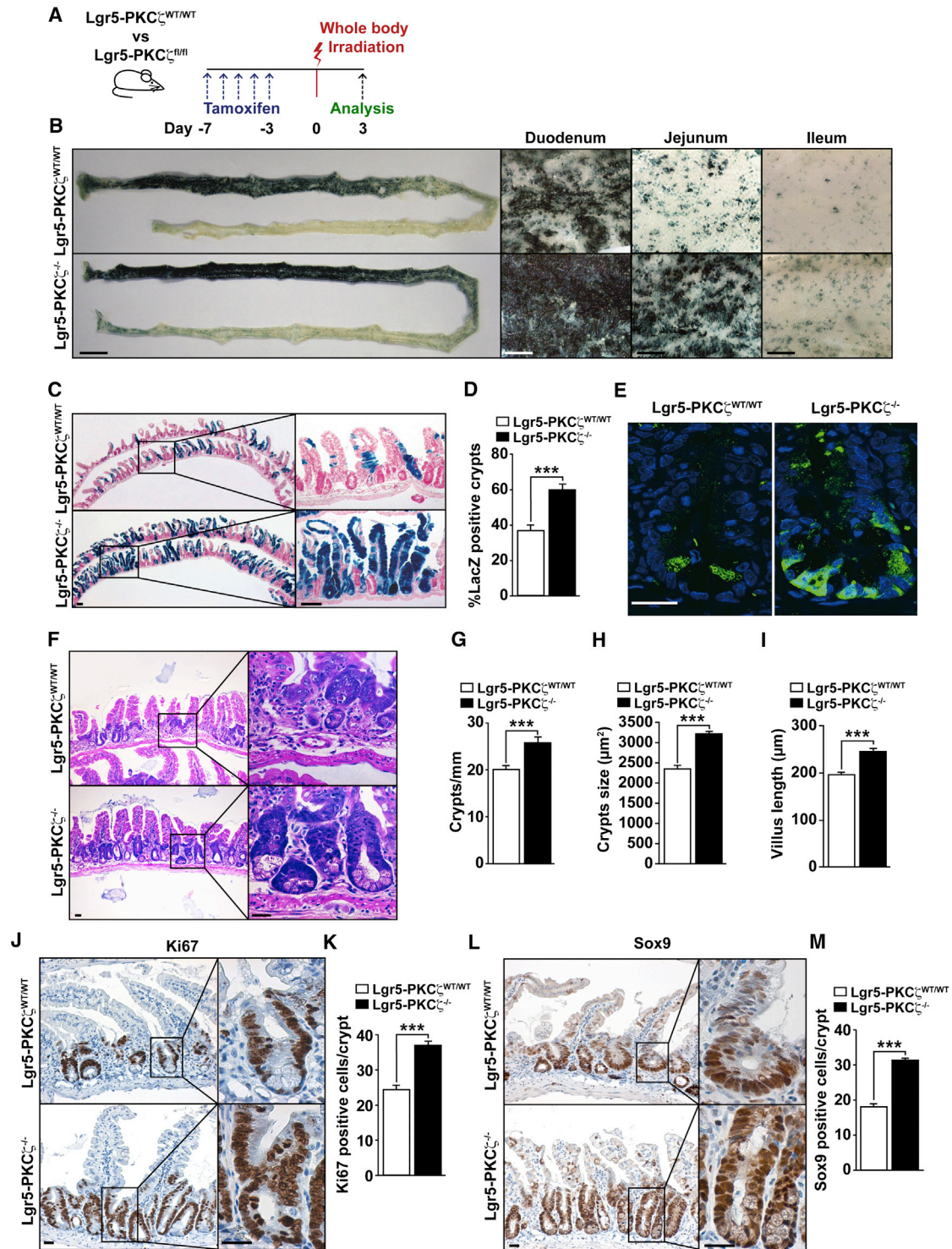


**Figure 2. PKC $\zeta$  Deficiency in Lgr5<sup>+</sup> Cells Leads to Improved Intestinal Regeneration**

(A) Experimental design.

(B) Macroscopic (left) and magnified (for duodenum, jejunum, and ileum) images of LacZ-stained small intestine in Lgr5-PKC $\zeta$ <sup>WT/WT</sup> and Lgr5-PKC $\zeta$ <sup>-/-</sup> mice 3 days after IR. Scale bars represent 1 cm (macroscopic) and 1 mm (magnified).

(C–E) LacZ staining of small intestine; scale bars represent 100  $\mu\text{m}$  (C); quantification of the number of LacZ positive crypts (D) and GFP staining labeling Lgr5<sup>+</sup> cells; scale bars represent 25  $\mu\text{m}$  (E) from irradiated Lgr5-PKC $\zeta$ <sup>WT/WT</sup> and Lgr5-PKC $\zeta$ <sup>-/-</sup> mice.

(F) H&E-stained sections of small intestine from Lgr5-PKC $\zeta$ <sup>WT/WT</sup> and Lgr5-PKC $\zeta$ <sup>-/-</sup> mice 3 days after IR. Scale bars represent 25  $\mu\text{m}$ .

(legend continued on next page)

These two GFP-positive populations were sorted and separated from the LGR5-GFP-negative fraction (GFP<sup>neg</sup>), after which mRNA was extracted from the different cell populations and analyzed by qRT-PCR to determine PKC $\zeta$  content. Interestingly, PKC $\zeta$  was expressed in the three cell fractions and highly enriched in the GFP<sup>lo</sup> cell population (Figure 1C). Consistent with these results, immunofluorescence staining of PKC $\zeta$  showed apical localization in epithelial cells in the crypt, including colocalization with crypt bottom stem cells with strong GFP expression (Figure 1D). The fact that PKC $\zeta$  was relatively enriched in the GFP<sup>lo</sup> population as compared to the GFP<sup>hi</sup> would suggest its potential stem cell-suppressor activity. Therefore, to determine whether PKC $\zeta$  deficiency in fact influences ISC activity, we carried out experiments in an organoid culture model system using intestinal crypts from wild-type (WT) or total-body PKC $\zeta$  knockout (PKC $\zeta$  KO) mice. This system assesses the activity of ISCs on the basis of their ability to drive the formation of organoids. Interestingly, PKC $\zeta$  deficiency led to increases in both the number and complexity (higher number of lobes) of intestinal organoids (Figures 1E–1G), strongly indicating that PKC $\zeta$ 's role is to restrain the activity of ISCs. Consistent with this, gene transcripts of the stem cell markers *Lgr5* and *Bmi1* were upregulated in PKC $\zeta$ -deficient organoids as compared to WT controls (Figure 1H). Similar increases in these markers were found in isolated intestinal epithelial cells (IECs) and in extracts from small intestine of PKC $\zeta$  KO mice (Figures 1I and 1J).

We next used the *Lgr5*Cre-Rosa26-LacZ knockin model described above, but bred into a PKC $\zeta$  KO background. In this system, injection of tamoxifen allows the stem cell progeny to be followed by X-gal staining. Notably, PKC $\zeta$  KO intestines had increased numbers of LacZ-stained cells, as compared with WT controls (Figures 1K–1M). Staining appeared along the flanks of the crypt-villus units of PKC $\zeta$ -deficient intestines at day 5 after tamoxifen injection to a greater extent than in WT mice (Figures 1K–1M). This is in agreement with the idea that the loss of PKC $\zeta$  favors increased stem cell activity in the intestine. Interestingly, staining of these samples with markers of differentiated cell populations such as enterocytes (Figure S1A), Goblet (Figure S1B), or Paneth (Figure S1C) cells did not show differences between the two mouse genotypes. Also, no major alterations were detected in polarity in PKC $\zeta$  KO intestines when several markers were analyzed by qRT-PCR or by immunohistochemistry of E-cadherin, Na/K-ATPase, or ZO-1 (Figures S1D–S1F), supporting the notion that the stem cell repressor activity of PKC $\zeta$  is not related to regulation of intestine epithelial cell polarity.

### PKC $\zeta$ Deficiency Promotes Intestinal Regeneration

Stem cells play a central role in intestinal regeneration after acute damage, which can be modeled by irradiation (IR)-induced ablation of the intestinal epithelium. To definitively establish the role of PKC $\zeta$  in the *Lgr5*<sup>+</sup> stem cell population and to rule out the hypothetical contribution of cells other than *Lgr5*<sup>+</sup>, we generated

mice with PKC $\zeta$  KO only in the *Lgr5*<sup>+</sup> stem cell population. For this, we crossed *Lgr5*Cre-Rosa26-LacZ mice with a mouse line with floxed PKC $\zeta$  alleles (PKC $\zeta$ <sup>fl/fl</sup>). In the resulting progeny, termed *Lgr5*-PKC $\zeta$ <sup>fl/fl</sup>, PKC $\zeta$  was deleted selectively in *Lgr5*<sup>+</sup> cells upon tamoxifen injection, thus generating *Lgr5*-PKC $\zeta$ <sup>-/-</sup> mice. As above, this manipulation also made possible the in vivo tracking and determination of the subsequent fate of these *Lgr5*<sup>+</sup> cells by X-gal staining. Therefore, *Lgr5*-PKC $\zeta$ <sup>WT/WT</sup> and *Lgr5*-PKC $\zeta$ <sup>fl/fl</sup> mice were injected with tamoxifen and irradiated 7 days thereafter. Afterward, they were allowed to recover and analyzed 3 days post-IR (Figure 2A). Whole-mount X-gal staining revealed increased signal in the intestines of *Lgr5*-PKC $\zeta$ <sup>-/-</sup> mice, as compared with *Lgr5*-PKC $\zeta$ <sup>WT/WT</sup> mice (Figure 2B). Histology also demonstrated increased regeneration of the *Lgr5*-expressing population in the *Lgr5*-PKC $\zeta$ <sup>-/-</sup> intestines, as documented by a strong increase in LacZ-labeled crypt-villus units (Figures 2C and 2D) and increased number of GFP-positive cells (Figure 2E). Furthermore, we found that crypt number and size and villus length were increased in *Lgr5*-PKC $\zeta$ <sup>-/-</sup> mice as compared to WT mice after IR (Figures 2F–2I). We also found increased Ki67 (Figures 2J and 2K) and Sox9 (Figures 2L and 2M) staining in the crypts of *Lgr5*-PKC $\zeta$ <sup>-/-</sup> intestines as compared with identically treated *Lgr5*-PKC $\zeta$ <sup>WT/WT</sup> mice. These results are consistent with a specific role for PKC $\zeta$  in the repopulation potential of ISCs.

### Selective PKC $\zeta$ Deficiency in *Lgr5*<sup>+</sup> Stem Cells Promotes Intestinal Tumorigenesis

Dysregulation of stem cell activity by such as deletion of the tumor suppressor gene *Apc* has been associated with intestinal tumorigenesis in several systems (Barker et al., 2009). To determine whether the selective loss of PKC $\zeta$  in *Lgr5*<sup>+</sup> ISCs enhances tumor-forming potential from these cells, we crossed *Lgr5*-PKC $\zeta$ <sup>WT/WT</sup> and *Lgr5*-PKC $\zeta$ <sup>fl/fl</sup> mice with *APC*<sup>fl/fl</sup> mice. These mice were subsequently injected with tamoxifen as described in Figure 3A, which generated *Lgr5*-PKC $\zeta$ <sup>WT/WT/APC</sup><sup>-/-</sup> and *Lgr5*-PKC $\zeta$ <sup>-/-/APC</sup><sup>-/-</sup> mouse lines. Mice of the different genotypes were then analyzed for tumor formation 16 days postinjection. Consistent with previously published data (Barker et al., 2009), the loss of APC in the *Lgr5* population efficiently drove the induction of adenomas in the small intestine (Figure 3B). Interestingly, the number and size of these tumors were dramatically increased by the simultaneous deletion of APC and PKC $\zeta$  selectively in *Lgr5* stem cells (Figures 3B–3E). In addition, the lack of PKC $\zeta$  in *Lgr5*<sup>+</sup> cells enhanced tumor aggressiveness. That is, whereas *Lgr5*-PKC $\zeta$ <sup>WT/WT/APC</sup><sup>-/-</sup> mice only showed low-grade adenomas with hyperchromatism of nuclei, tumors generated from *Lgr5*-PKC $\zeta$ <sup>-/-/APC</sup><sup>-/-</sup> mice corresponded to high-grade adenomas, with nuclear atypia and marked architectural distortion, including some areas consistent with intramucosal adenocarcinoma, characterized by a cribriform pattern of growth and an expanding-type infiltration into the lamina propria (Figure 3F). In addition, a similar phenotype was found in the

(G–I) Number of crypts per millimeter (G), crypt size (H), and villus length (I).

(J and K) Images (J) and quantification (K) of Ki67 staining of *Lgr5*-PKC $\zeta$ <sup>WT/WT</sup> and *Lgr5*-PKC $\zeta$ <sup>-/-</sup> small intestines 3 days after IR. Scale bars represent 25  $\mu$ m.

(L and M) Images (L) and quantification (M) of Sox9 staining of small intestine from irradiated *Lgr5*-PKC $\zeta$ <sup>WT/WT</sup> and *Lgr5*-PKC $\zeta$ <sup>-/-</sup> mice.

Scale bars represent 25  $\mu$ m. Results are presented as mean  $\pm$  SEM. Counts are of at least 20 fields of view per mouse (n = 4 mice). \*\*\*p < 0.001.

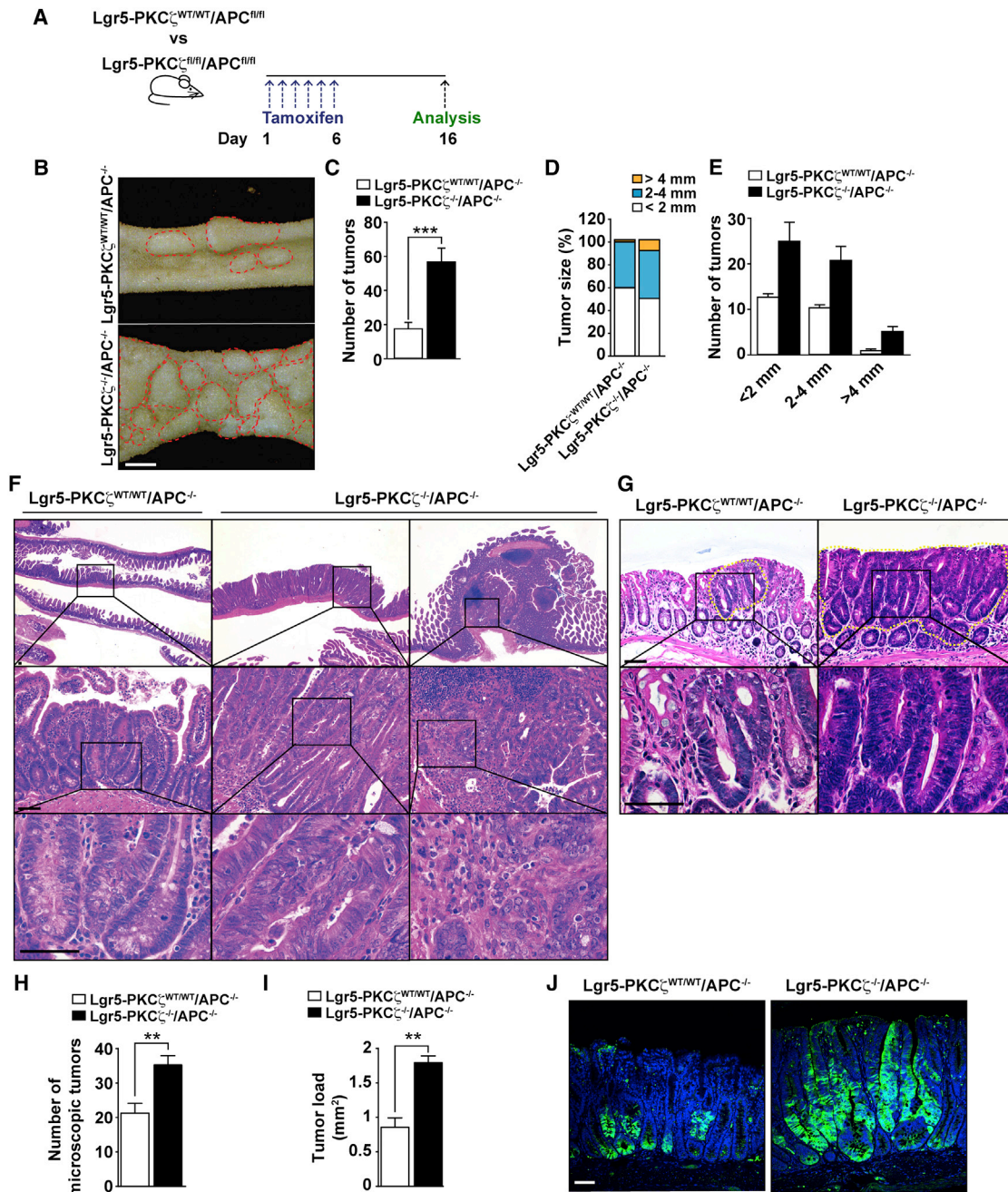


**Figure 3. PKC $\zeta$  Deletion in Lgr5<sup>+</sup> Cells Enhances Intestinal Tumorigenesis**

(A) Experimental design.  
 (B) Tumors (red circles) from Lgr5-PKC $\zeta^{WT/WT}/APC^{-/-}$  and Lgr5-PKC $\zeta^{-/-}/APC^{-/-}$  16 days after tamoxifen injection. Scale bars represent 2 mm.  
 (C) Quantification of the total number of tumors per mouse (n = 7).  
 (D) Tumor size distribution.  
 (E) Stratification of number of tumors according to size.  
 (F) H&E-stained sections of intestine from both genotypes, showing an adenoma with low-grade dysplasia in Lgr5-PKC $\zeta^{WT/WT}/APC^{-/-}$  mice (left panels) and adenoma with high-grade dysplasia or intramucosal adenocarcinoma in Lgr5-PKC $\zeta^{-/-}/APC^{-/-}$  mice (middle and right panels, respectively). Scale bar represents 50  $\mu$ m.  
 (G) H&E staining of colon tumors (yellow dash circles) from both genotypes, showing a large and highly dysplastic tumor in Lgr5-PKC $\zeta^{-/-}/APC^{-/-}$  mice as compared to Lgr5-PKC $\zeta^{WT/WT}/APC^{-/-}$  mice. Scale bar represents 50  $\mu$ m.  
 (H and I) Tumor numbers (H) and tumor load (I) (n = 7).  
 (J) GFP staining, labeling Lgr5<sup>+</sup> cells, of tumors from both genotypes. Scale bar represents 25  $\mu$ m.  
 Results are presented as mean  $\pm$  SEM. \*\*p < 0.01, \*\*\*p < 0.001.

colon of *Lgr5-PKCζ<sup>-/-</sup>/APC<sup>-/-</sup>* mice that displayed bigger and more dysplastic tumors, with increased number and load of colon tumors as compared to *Lgr5-PKCζ<sup>WT/WT</sup>/APC<sup>-/-</sup>* mice (Figures 3G–3I). Interestingly, GFP staining, a surrogate marker of *Lgr5<sup>+</sup>* stem cell activity in these mice, demonstrated that the loss of *PKCζ* in *Lgr5<sup>+</sup>* cells promotes stem cell activity along the large part of the tumors whereas *Lgr5<sup>+</sup>* cells that are WT for *PKCζ* retain the staining in a small population of cells, corresponding only with the base of the dysplastic crypts (Figure 3G). Collectively, these results demonstrate that *PKCζ* deficiency promotes ISC activity that translates into increased tumorigenesis.

### Low *PKCζ* Expression in Human Colon Adenocarcinoma Correlates with Stem Cell and YAP/ $\beta$ -Catenin Signatures

To assess the relevance of these findings to human disease, we performed gene set enrichment analysis (GSEA) of human colon adenocarcinoma samples using data obtained from The Cancer Genome Atlas Network (COAD data set) using the C2 Molecular Signatures Database (MSigDB, Broad Institute) to find gene expression signatures that correlated with *PKCζ* expression. Notably, and consistent with our *in vivo* mouse model data, we found that human colon adenocarcinoma tumors with low levels of *PKCζ* mRNA exhibited transcriptional profiles associated with an enrichment of stem cell signatures (Figure 4A). Also, *PKCζ* mRNA levels negatively correlated in these human tumors with the stem cell marker genes *Hopx* and *Bmi1* (Figure 4B). These results support the mouse studies demonstrating that *PKCζ* restrains tumorigenesis by inhibiting ISC activity and are consistent with data showing that patients with low *PKCζ* levels or high expression of stem cell genes have a significantly worse prognosis (Ma et al., 2013; Merlos-Suárez et al., 2011).

To start addressing the potential signaling mechanisms regulated by *PKCζ* in ISCs, we extended the GSEA analysis of the COAD data set using the C6 MSigDB that includes oncogenic signatures of signaling pathways deregulated in cancer. Of potential great relevance, this analysis revealed that low *PKCζ* expression correlated with enrichment in Yap signaling (Figure 4C). Furthermore, we found a significant inverse correlation between *PKCζ* gene expression levels and those of Yap target genes such as *CTGF* and *Cyr61* (Figure 4D). In addition, colon adenocarcinoma patients with low *PKCζ* expression displayed significantly higher levels of Yap (Figure 4D). In line with these results, GSEA of a transcriptomic profiling of the human colorectal adenocarcinoma cell line SW480 with knockdown of *PKCζ* (*shPKCζ*) also identified “Yap\_up” as significantly enriched in *PKCζ*-deficient cells as compared to nontargeted control cells (*shNT*) (Figure 4E). This suggests that *PKCζ*'s mechanism of action could involve the repression of Yap signaling. Interestingly, Ingenuity Pathway Analysis of the same transcriptome revealed that the most significantly enriched genes in *PKCζ*-deficient SW480 cells as compared to the *PKCζ*-proficient controls fell in the canonical pathway category of “Wnt/ $\beta$ -catenin signaling,” with significant upregulation of  $\beta$ -catenin target genes (Figure 4F). Importantly, *PKCζ* levels displayed a significant inverse correlation with the  $\beta$ -catenin-dependent gene *CD44* in human colon adenocarcinoma tumors (Figure 4G). In addition, these re-

sults are in good agreement with those obtained in a parallel effort using small interfering RNA (siRNA) screening to identify potential targets of *PKCζ* in SW480 cells. Thus, when this screening was carried with a pooled siRNA library covering 252 components of major oncogenic pathways designed to identify genes that had a differential impact on the viability of *PKCζ*-deficient SW480 as compared to *shNT* control cells, we found  $\beta$ -catenin as the top hit in the screen (Figure 4H; Table S1). It should be noted that the Yap pathway was not included in the siRNA set used in this screening (Table S1). Collectively, the clinical data, together with the unbiased transcriptomic and functional genomic approaches, strongly suggest that Yap and  $\beta$ -catenin are potential targets of *PKCζ* function.

### *PKCζ* Deficiency Results in Enhanced $\beta$ -Catenin and Yap Signaling

To investigate whether *PKCζ* represses ISC function through the regulation of  $\beta$ -catenin and Yap signaling, we first determined the expression of transcripts involved in these pathways upon deficiency of *PKCζ* in the *in vivo* mouse models. Notably, we found that well established target genes of  $\beta$ -catenin and Yap, including Yap itself, were significantly upregulated in organoids (Figure 5A), IECs (Figure 5B), and small intestine extracts (Figure 5C) from *PKCζ* KO mice kept under basal conditions, as compared with WT controls. Furthermore, analysis of mRNA levels of *Axin-2* and *CTGF*, targets of  $\beta$ -catenin and Yap, respectively, in the sorted GFP populations of Figure 1B, also revealed that both transcripts were reduced in the GFP<sup>lo</sup> population in which *PKCζ* levels were enriched (Figures 1B and 1C). This is in keeping with the repression of these pathways by *PKCζ* (Figure S2A). In addition, *PKCζ*-deficient intestines displayed increased nuclear Yap staining (Figures 5D and 5E). Likewise, staining of *CD44*, a downstream target of the Wnt/ $\beta$ -catenin pathway, was more intense and widespread in the mutant intestines (Figure 5F). Furthermore, immunoblot analysis showed increased  $\beta$ -catenin and Yap protein levels in IECs from *PKCζ* KO mice (Figure 5G). Notably, Yap protein levels were also increased in IECs from *Lgr5-PKCζ<sup>-/-</sup>* mice, as well as in organoid cultures from *PKCζ* KO mice (Figure 5H). Similar results were obtained when IECs and tissues from IR-treated mice were analyzed for expression of Yap- or  $\beta$ -catenin-target genes (Figures S2B–S2E). Altogether, these results strongly suggest that *PKCζ* is a direct or indirect negative regulator of  $\beta$ -catenin and Yap pathways, two important mediators in stem cell function.

### Yap and $\beta$ -Catenin Are Direct Substrates of *PKCζ*

We next investigated the molecular mechanisms whereby *PKCζ* specifically represses Yap and  $\beta$ -catenin. First, we found that *PKCζ* interacted with Yap and  $\beta$ -catenin in cotransfection experiments (Figures 6A and 6B). Also, *in vitro* interaction assays using purified recombinant proteins demonstrate that the interaction of *PKCζ* with Yap and  $\beta$ -catenin was direct (Figure 6C). We also detected this interaction in immunoprecipitates of endogenous proteins (Figure 6D). More importantly, immunoprecipitation of endogenous *PKCζ* pulled down not only Yap and  $\beta$ -catenin but also *GSK3 $\beta$*  and *Axin1* (Figure 6D). These results suggest that *PKCζ* is part of the  $\beta$ -catenin

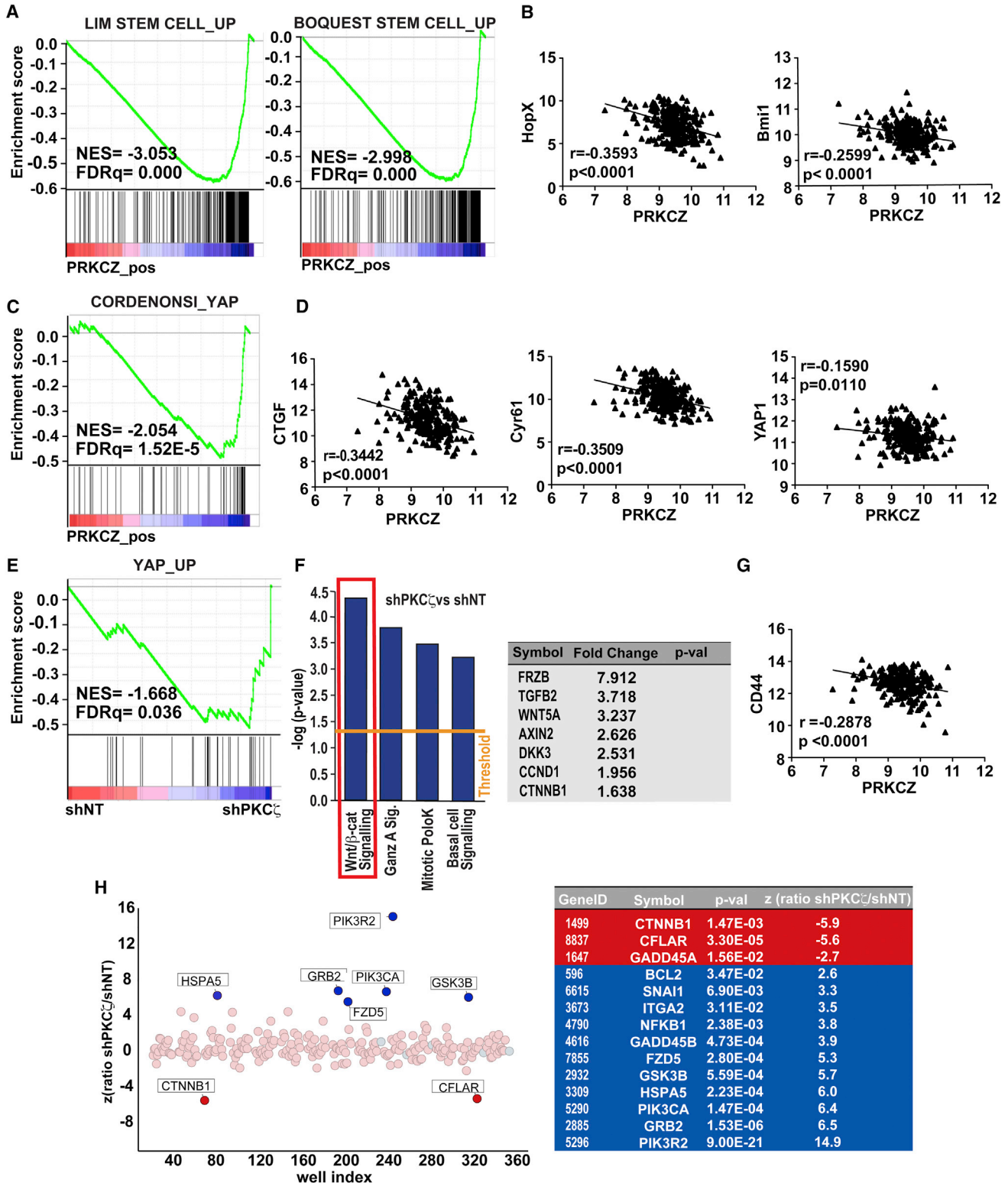


**Figure 4. PKC $\zeta$  Is Inversely Associated with Stemness and Yap/ $\beta$ -Catenin Signaling in Human Colon Adenocarcinomas**

(A) GSEA plots of enrichment in stem cell signatures in low PKC $\zeta$  expressing-tumors from human colon adenocarcinomas from The Cancer Genome Atlas COAD data set using C2 MSigDB database.

(B) Negative correlation between mRNA levels of PKC $\zeta$  and stem cell markers (Bmi1 and Hopx) in the same data set as in (A).

(legend continued on next page)



destruction complex in which Axin1 acts as a scaffold protein orchestrating the phosphorylation and degradation of  $\beta$ -catenin (Li et al., 2012). To more firmly establish this question, we treated HEK293T cells with Wnt3a and analyzed the potential recruitment of PKC $\zeta$  to the Axin complex. It is well established that cell activation by Wnt results in the degradation of Axin1, which correlates with  $\beta$ -catenin stabilization (Li et al., 2012; Mao et al., 2001; Tolwinski et al., 2003). Interestingly, Axin1 was degraded and the coimmunoprecipitation with PKC $\zeta$  and GSK3 $\beta$  was reduced upon Wnt3a stimulation (Figure 6E). These results indicate that PKC $\zeta$  is a bona fide component of the Axin1 complex and therefore could be involved in the regulation of  $\beta$ -catenin stability and function.

Given that Yap and  $\beta$ -catenin directly bind PKC $\zeta$ , a potential mechanism whereby PKC $\zeta$  impacts their function could be through direct phosphorylation. Therefore, we tested whether Yap and/or  $\beta$ -catenin could be phosphorylated by PKC $\zeta$ , using an in vitro phosphorylation assay with recombinant PKC $\zeta$  and purified bacterially expressed Yap and  $\beta$ -catenin. The results of this experiment demonstrated that in fact Yap and  $\beta$ -catenin are direct substrates of PKC $\zeta$  (Figures 6F and 6G). To map the phosphorylated sites in Yap and  $\beta$ -catenin, we used titanium dioxide (TiO<sub>2</sub>)-based phosphopeptide enrichment on tryptic digests of in vitro phosphorylation reactions followed by high-performance liquid chromatography tandem mass spectrometry (MS/MS) analysis. Using this approach, we identified S109 and T110 as major PKC $\zeta$  phosphorylation sites in Yap and several sites of low abundance that included T119, S163, and S164 (Figure S3A). To assess the relative contribution of sites S109 and T110, we performed an ATP analog-based in vitro phosphorylation assay with PKC $\zeta$  using recombinant WT- or S109A/T110A-Yap as substrates (Figure 6H). Consistent with MS/MS analysis, mutation to alanine of these two sites completely abolished Yap phosphorylation by PKC $\zeta$ . Interestingly, S109 and T110 sites were highly conserved among species (Figure S3B), which suggested an important role in Yap regulation.

Similar MS/MS analysis to map the sites phosphorylated in  $\beta$ -catenin by PKC $\zeta$  identified S45 and several sites of low abundance that included S552 and S675 (Figure S3C). S45, along with S33, S37, and T41 at the amino-terminal region of  $\beta$ -catenin, conforms to the consensus GSK3 phosphorylation sequence and, when phosphorylated, is critical for the recognition of  $\beta$ -catenin by the F box protein  $\beta$ -Trcp, which is an essential step for its ubiquitination and subsequent proteasome-mediated degradation (Clevers, 2013; Niehrs, 2012). Importantly, phosphorylation of  $\beta$ -catenin's S45 precedes, and is required for, subsequent GSK3-mediated phosphorylation of S33, S37, and T41 and the ensuing degradation of  $\beta$ -catenin. Interestingly, in vitro phos-

phorylation assays followed by immunoblotting with a specific anti-phospho-S45- $\beta$ -catenin antibody confirmed that S45 is a bona fide phosphorylation site of PKC $\zeta$  in  $\beta$ -catenin (Figure 6I). More importantly, immunoblotting of IEC extracts from Lgr5-PKC $\zeta^{-/-}$  and WT mice, and organoid extracts from WT and PKC $\zeta$  KO mice demonstrated that the loss of PKC $\zeta$  resulted in a profound inhibition of  $\beta$ -catenin phosphorylation at S45, concomitant with the accumulation of total  $\beta$ -catenin levels (Figures 6J and 6K). In contrast, analysis of IEC and organoid extracts revealed that in vivo PKC $\zeta$  deficiency did not inhibit  $\beta$ -catenin phosphorylation at S552 and S675 (Figures 6J and 6K), consistent with the finding that these sites were found in low abundance in the MS/MS proteomic analysis in vitro.

### PKC $\zeta$ Regulates Protein Stability and Function of Yap and $\beta$ -Catenin by Phosphorylation

To determine the functional relevance of Yap and  $\beta$ -catenin phosphorylation by PKC $\zeta$ , either WT or the nonphosphorylatable Yap S109A/T110A mutant was expressed along with increasing amounts PKC $\zeta$ , after which we assessed the effect of PKC $\zeta$  expression on the activity of Yap by using a TEAD-luciferase reporter. Notably, expression of either WT or mutant Yap was able to activate the TEAD-luciferase reporter to a similar extent (Figure 7A). However, the coexpression of PKC $\zeta$  resulted in inhibition of the TEAD-reporter activity induced by WT Yap, but not by mutant Yap (Figure 7A). This demonstrates that Yap function is directly regulated by phosphorylation in residues S109/T110.

Of note, Yap function is restrained through phosphorylation by the Hippo kinases Mst1/2 and Lats (Barry and Camargo, 2013; Mo et al., 2014). Therefore, we tested whether Yap constructs containing mutations in the Mst or Lats phosphorylation sites, termed 2SA (S127/381A) and Yap5SA (S61/109/127/164/381), were also sensitive to PKC $\zeta$ 's actions. Results of Figure S4A demonstrate that overexpression of PKC $\zeta$  was able to restrain TEAD-activity induced by Yap2SA with no effect on the activity of Yap5SA (Figure S4A). These data are consistent with the fact that the S109 phosphorylation site by PKC $\zeta$  is also mutated in the Yap5SA mutant, but not in the Yap2SA mutant, further reinforcing the notion that PKC $\zeta$  targets Yap at S109/T110 and in a manner that is likely independent of the Hippo/Mst cascade. Collectively, these results are consistent with our in vivo data shown above (Figures 5A–5D), demonstrating that PKC $\zeta$  deficiency resulted in increased Yap activity.

Interestingly, the levels of WT Yap, but not of the S109A/T110A mutant, were decreased by coexpression of PKC $\zeta$  (Figure 7A), demonstrating that this kinase regulates Yap transcriptional activity by controlling Yap levels through direct phosphorylation.

(C) GSEA plot of enrichment in Yap signature in low PKC $\zeta$  expressing-tumors from COAD data set using C6 MSigDB database.

(D) Inverse correlation of Yap-related genes in same data set as (A).

(E) GSEA plot of Yap signaling associated with gene expression in shPKC $\zeta$ -SW480 cells (GSE42186).

(F) Ingenuity Pathway analysis of the transcriptome of shPKC $\zeta$ -SW480 cells as compared to shNT control cells (left panel). Wnt/ $\beta$ -catenin target genes upregulated in shPKC $\zeta$ -SW480 cells (right panel).

(G) Negative correlation between PKC $\zeta$  and the  $\beta$ -catenin target gene, CD44, in the COAD data set.

(H) siRNA screening of genes required for shPKC $\zeta$ -SW480 cell survival compared to shNT cells. A differential viability ratio shPKC $\zeta$ /NT was computed for each gene to derive the Z score. Light red dots, library siRNA pools; light blue dots, negative control pool. Positive Z values indicate genes preferentially required for the control line viability; negative Z values indicate genes preferentially required for shPKC $\zeta$  line viability. List of highly significant hits are shown. See also Table S1.

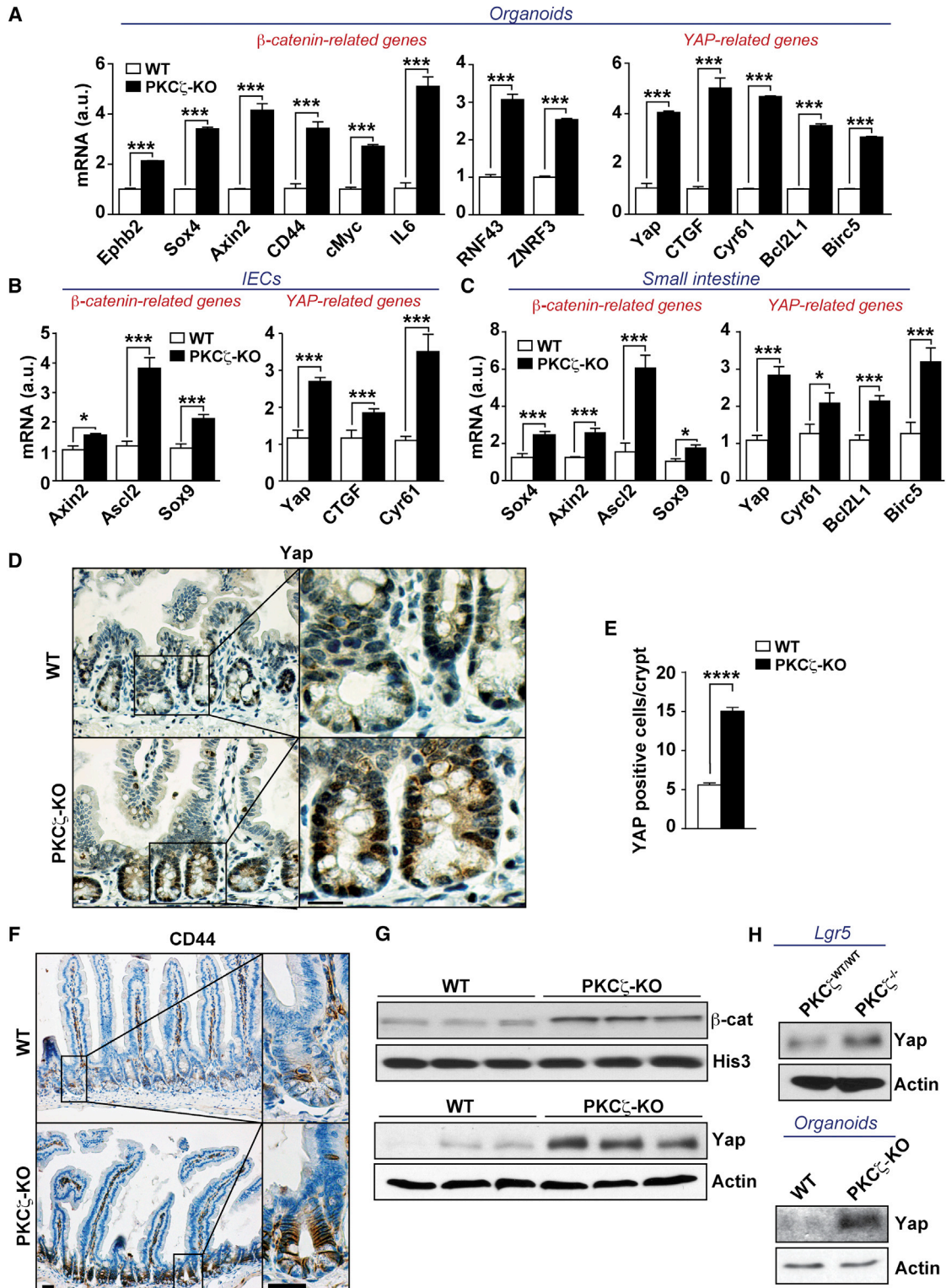


**Figure 5. PKC $\zeta$  Deficiency Results in Enhanced  $\beta$ -Catenin and Yap Signaling**

(A–C) mRNA levels of Wnt/ $\beta$ -catenin- and Yap-related genes in crypt organoids (n = 3) after 3 days in culture (A), isolated intestinal epithelial cells (IECs) (n = 6) (B), and small intestine (n = 6) of WT and PKC $\zeta$  KO mice (C).

(D and E) Yap staining (D) and quantification (E) in small intestine from WT and PKC $\zeta$  KO mice (n = 6).

(F) CD44 staining of small intestine from WT and PKC $\zeta$  KO mice (n = 6).

(legend continued on next page)

This is consistent with our observations that Yap itself was upregulated in PKC $\zeta$ -deficient tissues in vivo (Figures 5D–5H). In keeping with this conclusion, the S109A/T110A Yap mutant was significantly more stable than WT Yap in cycloheximide-treated cells (Figure 7B), lending support to our hypothesis that PKC $\zeta$  represses Yap function by promoting its destabilization through direct phosphorylation of residues S109 and T110. Next, we determined the functional relevance of  $\beta$ -catenin phosphorylation at S45 by PKC $\zeta$ . Thus, we analyzed the effect of PKC $\zeta$  knockdown on  $\beta$ -catenin-induced transcriptional activity of a specific luciferase reporter construct termed TOPflash. In support of our hypothesis that PKC $\zeta$  is a negative regulator of the Wnt pathway, the ability of  $\beta$ -catenin to activate the TOPflash reporter was enhanced by PKC $\zeta$  knockdown (Figure 7C). In addition, expression of PKC $\zeta$  in cotransfection experiments resulted in the inhibition of TOPflash activity induced by WT  $\beta$ -catenin, but not by that of an S45A mutant, which correlated with decreased levels of WT  $\beta$ -catenin, but not the mutant protein, in the PKC $\zeta$ -expressing samples (Figures 7D and 7E). Collectively, these results establish PKC $\zeta$  as a negative regulator of  $\beta$ -catenin stability by phosphorylation of S45. Since this site has been shown to be a target of CK1 $\alpha$  (Clevers et al., 2014; Niehrs, 2012), we next determined whether its in vivo phosphorylation by PKC $\zeta$  is mediated by CK1 $\alpha$ . Interestingly, PKC $\zeta$ -induced depletion of  $\beta$ -catenin levels in vivo was not affected by the knockdown of CK1 $\alpha$  (Figure S4B). These results establish that S45 is a direct target of PKC $\zeta$  in a CK1 $\alpha$ -independent fashion.

Further supporting the functional relevance of PKC $\zeta$  regulation of  $\beta$ -catenin and Yap, we found that PKC $\zeta$  knockdown in SW480 colorectal carcinoma cells promotes the activation of the  $\beta$ -catenin and Yap reporters (Figures 7F and 7G). Notably, this correlated with increased levels of both transcriptional regulators in the PKC $\zeta$ -deficient cells (Figure 7H). Our previous studies in this system revealed the critical role of PKC $\zeta$  as a tumor suppressor in cancer cells undergoing nutrient stress (Ma et al., 2013). Therefore, we hypothesized that PKC $\zeta$  is a signaling molecule in the repression of both  $\beta$ -catenin and Yap in response to nutrient deprivation. Interestingly, incubation of PKC $\zeta$ -proficient SW480 cells under nutrient stress conditions inhibited the nuclear localization of  $\beta$ -catenin and Yap (Figure 7I). Importantly, this effect was completely abrogated in PKC $\zeta$ -deficient SW480 cells (Figure 7I). Consistently, the levels of  $\beta$ -catenin and Yap downstream transcripts were higher in PKC $\zeta$ -deficient SW480 cells under stress conditions than in the shNT controls (Figure S4C). Furthermore, knockdown of  $\beta$ -catenin or Yap inhibited the increased proliferation and survival of PKC $\zeta$ -deficient SW480 cells (Figure S4D). In order to establish the in vivo contribution of the  $\beta$ -catenin and Yap pathways to the mechanism of action of PKC $\zeta$ , we treated organoids from WT and PKC $\zeta$  KO mice with verteporfin, which inhibits Yap function by disrupting the Yap-TEAD interaction, or with a combination of DKK1 plus lwr1, which are inhibitors of the Wnt cascade. Consistent with

our hypothesis, the inhibition of both pathways rescued the phenotype of PKC $\zeta$  KO organoids (Figures 7J–7L).

## DISCUSSION

The identification of Lgr5<sup>+</sup> cells as an ISC population has expanded our understanding of the intestinal regeneration processes induced in response to acute injury and opens up new avenues for research on the role and mechanisms of action of the stem cells in cancer initiation (Barker et al., 2009). Since the intestinal epithelium has an inherently high cellular turnover, fueled by the activity of ISCs residing at the bottom of the crypts, it is difficult to envision how mutations could be passed along through successive generations if stem-cell-derived differentiated cells undergo apoptosis with a high frequency after terminal differentiation and are substituted by new epithelial cells. The existence of a pool of stem cells that could accumulate these mutations might account for the generation of tumors in the intestine and might offer possibilities for treatment as well as strategies for prevention of tumor initiation by blocking those pathways that are critical for the control of the stem-cell-driven carcinogenesis process (Anastas and Moon, 2013; Vermeulen and Snippert, 2014). Understanding the biochemistry and signaling properties of these intestinal Lgr5<sup>+</sup> stem cells will be instrumental in designing better strategies not only to prevent cancer but also to promote intestinal regeneration after acute or chronic damage, such as that triggered by chemoradiotherapies. Our recent results demonstrate that PKC $\zeta$  is a suppressor of tumor progression in intestinal carcinogenesis because it represses the ability of aggressive cancer cells to reprogram their metabolism under situations of nutrient stress in mouse and human cancers (Ma et al., 2013). We show here that PKC $\zeta$  deficiency leads to greater levels of stem cell activity in vitro and in vivo, which triggers an enhanced regenerative response to acute intestinal insults. Loss of PKC $\zeta$  also results in greater tumorigenic activity of the stem cell population in the absence of the tumor suppressor APC.

Although several signaling pathways are involved in intestine homeostasis and regeneration, including, BMP, Shh, and Notch, Wnt signaling has attracted great attention due to the fact that it is the target of several cancer-driving mutations (Clevers et al., 2014). Also, the Wnt/ $\beta$ -catenin cascade has been shown to be critical for the proliferation of ISCs and TA cells, as revealed by the lack of proliferative crypts in mice with deletion of its transcriptional partner Tcf4 (Korinek et al., 1998).  $\beta$ -Catenin is the effector of the Wnt pathway and is associated with, and degraded by, the APC/Axin/GSK3 $\beta$  complex (Clevers et al., 2014; Niehrs, 2012). Phosphorylation of  $\beta$ -catenin initially at S45 is a necessary event for GSK3 $\beta$  to sequentially phosphorylate residues S33, S37, and T41, creating a recognition motif for the E3-ligase  $\beta$ -Trcp that constitutively targets  $\beta$ -catenin for degradation (Clevers et al., 2014; Niehrs,

(G) Western blot of nuclear  $\beta$ -catenin or Yap levels of IECs from WT and PKC $\zeta$  KO mice (n = 3).

(H) Western blot of Yap levels in extracts from Lgr5-PKC $\zeta$ <sup>WT/WT</sup> and Lgr5-PKC $\zeta$ <sup>-/-</sup> mice 10 days after tamoxifen injection, and crypt organoids from WT and PKC $\zeta$  KO mice.

Scale bars represent 25  $\mu$ m. Results are representative of three experiments. Results are presented as mean  $\pm$  SEM. \*p < 0.05, \*\*p < 0.01, \*\*\*p < 0.001. See also Figure S2.

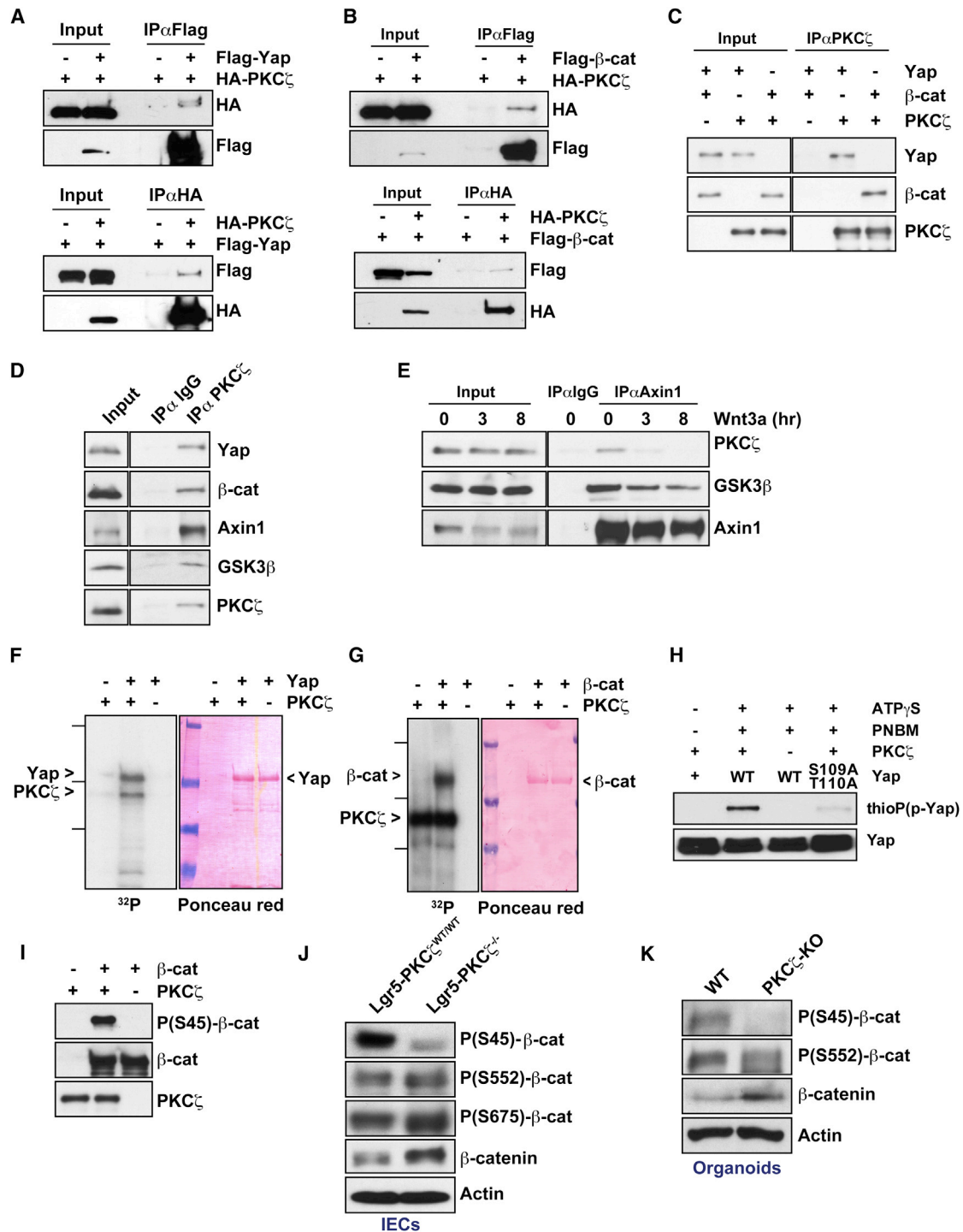


**Figure 6. Yap and  $\beta$ -Catenin Are Direct Substrates of PKC $\zeta$**

(A and B) Interaction of PKC $\zeta$  with Yap (A) and  $\beta$ -catenin (B) in cotransfection experiments in HEK293T cells. (C) In vitro interaction of recombinant PKC $\zeta$  with recombinant Yap and  $\beta$ -catenin. (D) Endogenous interaction of PKC $\zeta$  and components of Axin1 complex in HEK293T cells. (E) Endogenous association of Axin1 with PKC $\zeta$  and GSK3 $\beta$  in Wnt3a-treated HEK293T cells. (F and G) In vitro phosphorylation of Yap (F) and  $\beta$ -catenin (G) by PKC $\zeta$  with [ $\gamma$ - $^{32}$ P]-ATP. (H) Western blot of thiophosphate ester after YAP phosphorylation by PKC $\zeta$  with ATP $\gamma$ S. (legend continued on next page)

2012). Upon stimulation of the pathway, these phosphorylation events and the subsequent degradation of  $\beta$ -catenin are impaired, and  $\beta$ -catenin thus accumulates in the nucleus and activates the transcription of several critical components of the proliferation and stem cell activity (Clevers et al., 2014; Niehrs, 2012). Interestingly, we show here that PKC $\zeta$ 's role as a suppressor of tumorigenesis and ISC activity is mediated by the direct phosphorylation of S45 in a CK1 $\alpha$ -independent manner. Upon PKC $\zeta$  inactivation, which is common in human intestinal cancers and results in enhanced tumorigenesis in several mouse models (Ma et al., 2013),  $\beta$ -catenin becomes more stable and accumulates in the nucleus of intestinal epithelial and stem cells.

Along with Wnt/ $\beta$ -catenin, Yap has been proposed as an important regulator of ISC function (Clevers et al., 2014; Harvey et al., 2013; Mo et al., 2014). Yap is directly phosphorylated by the kinases Lats1/2 that are under regulation of the tumor suppressor Hippo pathway that includes the kinases Mst1 and Mst2 and the adaptor Sav1 (Harvey et al., 2013; Mo et al., 2014). Lats1/2-mediated phosphorylation of Yap S127 serves to promote its exclusion from the nucleus and its eventual degradation. Yap is expressed in both the small intestine and colon, displaying cytoplasmic localization in the upper regions of the crypt and villi whereas it is nuclear in the Lgr5<sup>+</sup> ISCs (Barry and Camargo, 2013). Even though the deletion of Yap has no significant effects on intestinal cell proliferation or function (Cai et al., 2010; Zhou et al., 2011), possibly due to the compensatory actions of Taz, its endogenous activation by inhibition of different components of the Hippo pathway in the intestine results in increased proliferation and tumorigenesis. That is, although overexpression Yap experiments *in vivo* gave contradictory results (Barry and Camargo, 2013; Li and Clevers, 2010), experiments modulating the endogenous levels of Yap strongly support its positive role in intestinal epithelial cell proliferation. Thus, deletion of both Mst1 and Mst2, whose role is to repress Yap function in the Hippo pathway, in the mouse intestine leads to crypt dysplasia in a Yap-dependent manner (Zhou et al., 2011). Furthermore, intestine-specific deletion of Sav1 in mice, which correlates with Yap activation, also leads to crypt hyperplasia with highly proliferating cells, a phenotype that is rescued by the concomitant inactivation of Yap (Cai et al., 2010). The link of Yap with intestinal cancer is apparent, since both double MST1/2 and Sav1 KO mice develop various forms of intestinal tumorigenesis (Cai et al., 2010; Zhou et al., 2011). Moreover, Yap and Taz expression is increased in colorectal cancer (CRC) patients (Cai et al., 2010; Steinhardt et al., 2008; Wang et al., 2013; Zhou et al., 2011), and it has been shown that Yap promotes resistance of CRC cells to chemotherapy (Touil et al., 2014). Therefore, our data shown here, demonstrating that PKC $\zeta$ , in addition to interacting with and phosphorylating  $\beta$ -catenin at S45, also binds Yap and promotes its phosphorylation at S109/T110 to impair its stability, is of great relevance in ISC function.

The fact that PKC $\zeta$  impinges in both pathways is of particular interest given the existence of a previously described crosstalk between Yap and  $\beta$ -catenin. In this regard, several studies have reported the interaction of Yap with different components of the Wnt pathway, including Dvl, Axin1, and  $\beta$ -catenin itself (Azzolin et al., 2014; Barry et al., 2013; Rosenbluh et al., 2012). The interaction with  $\beta$ -catenin is interesting because of the available data showing that Yap and  $\beta$ -catenin interact to promote cell survival and transformation of colon cancer cells (Rosenbluh et al., 2012). Since PKC $\zeta$  destabilizes both  $\beta$ -catenin and Yap levels and inhibits their transcriptional activity even when overexpressed, a situation that mimics their activation state, this suggests that PKC $\zeta$  actions will be relevant not only during  $\beta$ -catenin regulation by the destruction complex but also once this is inhibited. More interestingly, we show here that PKC $\zeta$  immunoprecipitation pulls down not only  $\beta$ -catenin and Yap but also Axin1, indicating that PKC $\zeta$  is also part of the destruction complex. Interestingly, recently published data showed that Yap/Taz are essential for the recruitment of  $\beta$ -TrCP to the Axin1 complex and subsequent  $\beta$ -catenin inactivation in cells under conditions of inactive Wnt (Azzolin et al., 2014). When cells are activated by Wnt, Yap/Taz are released from the complex and translocated to the nucleus (Azzolin et al., 2014). Under these conditions,  $\beta$ TrCP cannot be recruited to the complex and  $\beta$ -catenin, although phosphorylated, cannot be polyubiquitinated and degraded, clogging the destruction complex, which allows newly synthesized  $\beta$ -catenin to be translocated to the nucleus (Azzolin et al., 2014). Interestingly, cell stimulation with Wnt also promotes the degradation of Axin1 and therefore dislodges the destruction complex including the association with PKC $\zeta$  (Figures 6D and 6E). However, since PKC $\zeta$  directly binds  $\beta$ -catenin and Yap, this suggests that it regulates their stability probably when it is part of the destruction complex and also when released from Axin1, constituting an additional layer of control for  $\beta$ -catenin and Yap levels and functions.

In addition, our previously published data demonstrated that PKC $\zeta$  is part of a stress response triggered by nutrient deprivation, whereby PKC $\zeta$ 's role is to restrain survival of CRC cells under these conditions (Ma et al., 2013). In the present study, we show that PKC $\zeta$  deficiency prevents the inactivation of  $\beta$ -catenin and Yap by nutrient stress. This is in keeping with very recently reported evidence demonstrating that the Yap pathway is inhibited by energy stress through AMPK and the phosphorylation of AMOTL1 (DeRan et al., 2014). These results, together with our data, indicate that Yap and  $\beta$ -catenin are exquisitely regulated during situations of nutrient deprivation to ensure that these pathways are not activated when stem cells do not have the necessary conditions to survive when activated. As PKC $\zeta$  is a tumor suppressor, our model suggests that its role is to block tumorigenesis by preventing metabolic reprogramming under conditions of nutrient deprivation and by inhibiting the activation of  $\beta$ -catenin and Yap to block the stem cell activation programs, specially under conditions of stress.

(I) Western blot of S45- $\beta$ -catenin phosphorylated by PKC $\zeta$  *in vitro*.

(J and K) Western blot of  $\beta$ -catenin phosphorylation in IECs from Lgr5-PKC $\zeta^{WT/WT}$  and Lgr5-PKC $\zeta^{-/-}$  mice (J) and in crypt organoids from WT and PKC $\zeta$  KO mice (K).

Results are representative of three experiments. See also Figure S3.

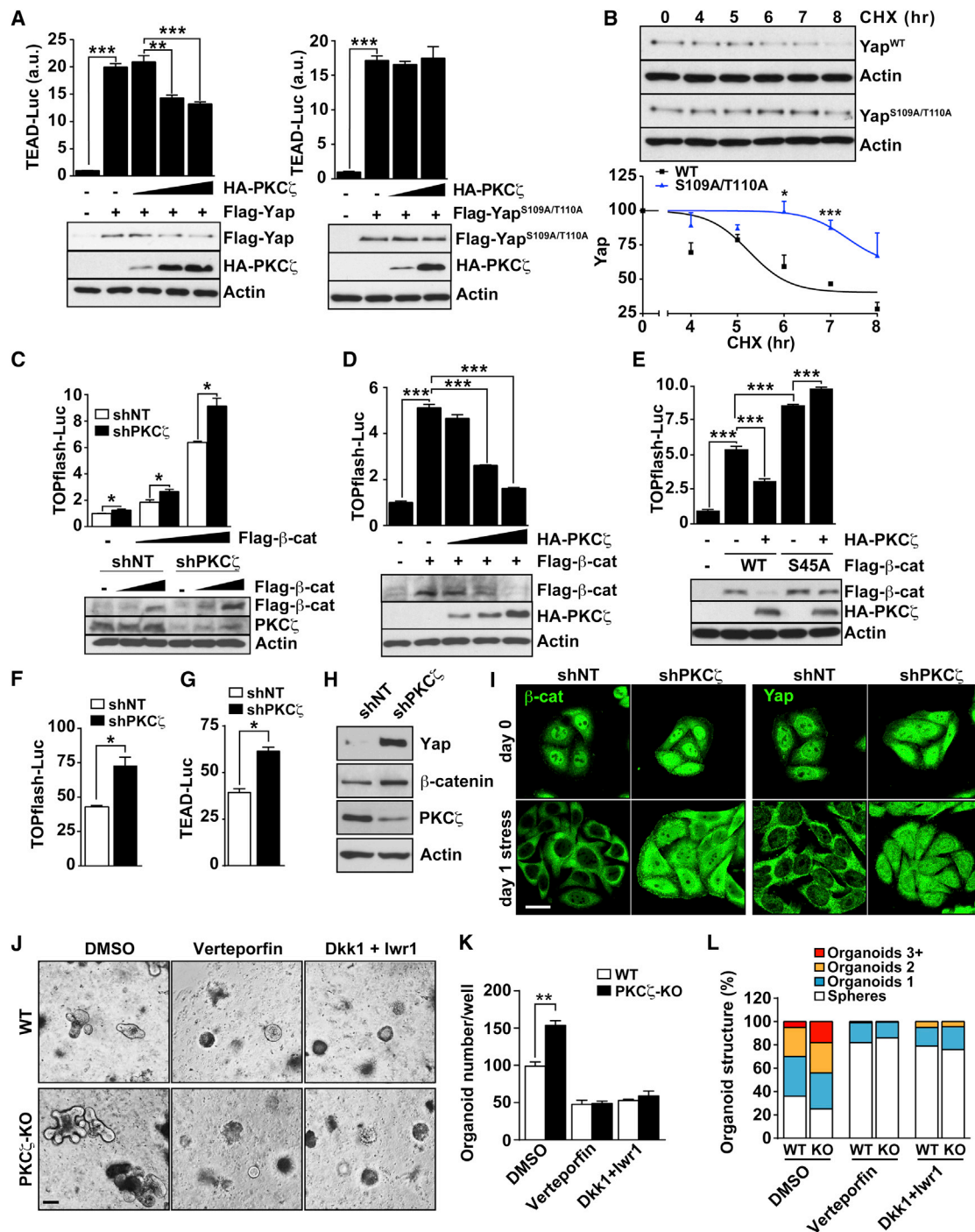


**Figure 7. PKC $\zeta$  Regulates the Stability and Function of Yap and  $\beta$ -Catenin**

(A) TEAD luciferase assay in HEK293T cells cotransfected with the indicated expression plasmids. Luciferase activity was normalized to Renilla activity. (B) HEK293T cells transfected with S109A/T110A Yap mutant or WT Yap were incubated with cycloheximide, and protein stability was determined by immunoblot. Yap protein levels were normalized to actin. (C) TOPflash-luciferase assay in shNT or shPKC $\zeta$ -HEK293T cells cotransfected with Flag- $\beta$ -catenin. Luciferase activity was normalized to Renilla activity (n = 3). (D and E) TOPflash-luciferase assay in HEK293T cells co-transfected with the indicated expression plasmids. Luciferase activity was normalized to Renilla activity (n = 3). (F and G) TOPflash (F) and TEAD (G) luciferase assays in shNT- or shPKC $\zeta$ -SW480 cells. Luciferase activity was normalized to Renilla activity (n = 3). (H) Western blot of extracts from shNT and shPKC $\zeta$  SW480 cells.

(legend continued on next page)

## EXPERIMENTAL PROCEDURES

### Mice

Animal handling and experimental procedures conformed to institutional guidelines (Sanford-Burnham Medical Research Institute Institutional Animal Care and Use Committee). PKC $\zeta$ <sup>fl/fl</sup> (Prkcz<sup>tm1a(EUCOMM)Wtsl</sup>) mice were obtained from the International Knockout Mouse Consortium and generated for the EUCOMM project by the Wellcome Trust Sanger Institute. Please see the [Supplemental Experimental Procedures](#) for more detailed protocols.

### IEC Isolation

Isolation of IECs was carried out as described previously (Egan et al., 2004).

### Statistical Analysis

Data are presented as the mean  $\pm$  SEM. Significant differences between groups were determined with a Student's t test (two tailed). The significance level for statistical testing was set at  $p < 0.05$ .

## SUPPLEMENTAL INFORMATION

Supplemental Information includes Supplemental Experimental Procedures, four figures, and two tables and can be found with this article online at <http://dx.doi.org/10.1016/j.celrep.2015.01.007>.

## AUTHOR CONTRIBUTIONS

V.L. and Y.N. performed most of experiments of this study with equal contribution. A.D. contributed to setting up the organoid system and sorting experiments. M.R.-C. and J.F. performed the phosphorylation experiments. M.R.-C. and P.M.S. contributed to the bioinformatic analysis. T.Y. generated phosphorylation mutants. A.C. performed the proteomic analysis. P.A. contributed to the siRNA screening. M.L. provided PKC $\zeta$  KO mice. M.T.D.-M. and J.M. conceived and supervised the project. M.T.D.-M. and J.M. wrote the manuscript with assistance from all the authors.

## ACKNOWLEDGMENTS

NIH grants R01CA132847 (J.M.), R01CA172025 (J.M.), R01CA134530 (M.T.D.-M.), and 5P30CA030199 (M.T.D.-M. and J.M.) funded this work. Additional support was provided by Department of Defense grants W81XWH-13-1-0353 (M.T.D.-M.) and W81XWH-13-1-0354 (J.M.). We thank Maryellen Daston for editing this manuscript, Diantha LaVine for the artwork, and Wei Liu and the personnel of the Flow Cytometry, Cell Imaging, Animal Facility, Histology, Proteomics, Functional Genomics, and Viral Vectors Shared Resources at SBMRI for technical assistance.

Received: September 19, 2014

Revised: December 10, 2014

Accepted: December 30, 2014

Published: February 5, 2015

## REFERENCES

Anastas, J.N., and Moon, R.T. (2013). WNT signalling pathways as therapeutic targets in cancer. *Nat. Rev. Cancer* **13**, 11–26.

Azzolin, L., Panciera, T., Soligo, S., Enzo, E., Bicciato, S., Dupont, S., Bresolin, S., Frasson, C., Basso, G., Guzzardo, V., et al. (2014). YAP/TAZ incorporation in the  $\beta$ -catenin destruction complex orchestrates the Wnt response. *Cell* **158**, 157–170.

Barker, N., van Es, J.H., Kuipers, J., Kujala, P., van den Born, M., Cozijnsen, M., Haegebarth, A., Korving, J., Begthel, H., Peters, P.J., and Clevers, H. (2007). Identification of stem cells in small intestine and colon by marker gene Lgr5. *Nature* **449**, 1003–1007.

Barker, N., Ridgway, R.A., van Es, J.H., van de Wetering, M., Begthel, H., van den Born, M., Danenberg, E., Clarke, A.R., Sansom, O.J., and Clevers, H. (2009). Crypt stem cells as the cells-of-origin of intestinal cancer. *Nature* **457**, 608–611.

Barry, E.R., and Camargo, F.D. (2013). The Hippo superhighway: signaling crossroads converging on the Hippo/Yap pathway in stem cells and development. *Curr. Opin. Cell Biol.* **25**, 247–253.

Barry, E.R., Morikawa, T., Butler, B.L., Shrestha, K., de la Rosa, R., Yan, K.S., Fuchs, C.S., Magness, S.T., Smits, R., Ogino, S., et al. (2013). Restriction of intestinal stem cell expansion and the regenerative response by YAP. *Nature* **493**, 106–110.

Cai, J., Zhang, N., Zheng, Y., de Wilde, R.F., Maitra, A., and Pan, D. (2010). The Hippo signaling pathway restricts the oncogenic potential of an intestinal regeneration program. *Genes Dev.* **24**, 2383–2388.

Clevers, H. (2013). The intestinal crypt, a prototype stem cell compartment. *Cell* **154**, 274–284.

Clevers, H., Loh, K.M., and Nusse, R. (2014). Stem cell signaling. An integral program for tissue renewal and regeneration: Wnt signaling and stem cell control. *Science* **346**, 1248012.

DeRan, M., Yang, J., Shen, C.H., Peters, E.C., Fitamant, J., Chan, P., Hsieh, M., Zhu, S., Asara, J.M., Zheng, B., et al. (2014). Energy stress regulates hippo-YAP signaling involving AMPK-mediated regulation of angiotensin-like 1 protein. *Cell Rep.* **9**, 495–503.

Egan, L.J., Eckmann, L., Gretchen, F.R., Chae, S., Li, Z.W., Myhre, G.M., Robine, S., Karin, M., and Kagnoff, M.F. (2004). IkappaB-kinasebeta-dependent NF-kappaB activation provides radioprotection to the intestinal epithelium. *Proc. Natl. Acad. Sci. USA* **101**, 2452–2457.

Galvez, A.S., Duran, A., Linares, J.F., Pathrose, P., Castilla, E.A., Abu-Baker, S., Leitges, M., Diaz-Meco, M.T., and Moscat, J. (2009). Protein kinase Czeta represses the interleukin-6 promoter and impairs tumorigenesis in vivo. *Mol. Cell Biol.* **29**, 104–115.

Harvey, K.F., Zhang, X., and Thomas, D.M. (2013). The Hippo pathway and human cancer. *Nat. Rev. Cancer* **13**, 246–257.

Korinek, V., Barker, N., Moerer, P., van Donselaar, E., Huls, G., Peters, P.J., and Clevers, H. (1998). Depletion of epithelial stem-cell compartments in the small intestine of mice lacking Tcf-4. *Nat. Genet.* **19**, 379–383.

Li, L., and Clevers, H. (2010). Coexistence of quiescent and active adult stem cells in mammals. *Science* **327**, 542–545.

Li, V.S., Ng, S.S., Boersema, P.J., Low, T.Y., Karthaus, W.R., Gerlach, J.P., Mohammed, S., Heck, A.J., Maurice, M.M., Mahmoudi, T., and Clevers, H. (2012). Wnt signaling through inhibition of  $\beta$ -catenin degradation in an intact Axin1 complex. *Cell* **149**, 1245–1256.

Ma, L., Tao, Y., Duran, A., Llado, V., Galvez, A., Barger, J.F., Castilla, E.A., Chen, J., Yajima, T., Porollo, A., et al. (2013). Control of nutrient stress-induced metabolic reprogramming by PKC $\zeta$  in tumorigenesis. *Cell* **152**, 599–611.

Mao, J., Wang, J., Liu, B., Pan, W., Farr, G.H., 3rd, Flynn, C., Yuan, H., Takada, S., Kimelman, D., Li, L., and Wu, D. (2001). Low-density lipoprotein receptor-related protein-5 binds to Axin and regulates the canonical Wnt signaling pathway. *Mol. Cell* **7**, 801–809.

Merlos-Suárez, A., Barriga, F.M., Jung, P., Iglesias, M., Céspedes, M.V., Rossell, D., Sevillano, M., Hernando-Mombalona, X., da Silva-Diz, V., Muñoz, P., et al. (2011). The intestinal stem cell signature identifies colorectal cancer stem cells and predicts disease relapse. *Cell Stem Cell* **8**, 511–524.

(I) Immunofluorescence of Yap and  $\beta$ -catenin in shNT and shPKC $\zeta$  SW480 cells in normal conditions or under nutrient-stress conditions. Scale bar represents 20  $\mu$ m.

(J–L) Images (J), quantification of number (K) and structural complexity (L) of WT- or PKC $\zeta$  KO mice-derived organoids treated with different inhibitors for 2 days in culture (n = 4).

Scale bar represents 200  $\mu$ m. Results are presented as mean  $\pm$  SEM. \* $p < 0.05$ , \*\* $p < 0.01$ , \*\*\* $p < 0.001$ . See also [Figure S4](#).

- Mo, J.S., Park, H.W., and Guan, K.L. (2014). The Hippo signaling pathway in stem cell biology and cancer. *EMBO Rep.* *15*, 642–656.
- Moscat, J., Diaz-Meco, M.T., and Wooten, M.W. (2009). Of the atypical PKCs, Par-4 and p62: recent understandings of the biology and pathology of a PB1-dominated complex. *Cell Death Differ.* *16*, 1426–1437.
- Niehrs, C. (2012). The complex world of WNT receptor signalling. *Nat. Rev. Mol. Cell Biol.* *13*, 767–779.
- Rosenbluh, J., Nijhawan, D., Cox, A.G., Li, X., Neal, J.T., Schafer, E.J., Zack, T.I., Wang, X., Tsherniak, A., Schinzel, A.C., et al. (2012).  $\beta$ -Catenin-driven cancers require a YAP1 transcriptional complex for survival and tumorigenesis. *Cell* *151*, 1457–1473.
- Schepers, A.G., Snippert, H.J., Stange, D.E., van den Born, M., van Es, J.H., van de Wetering, M., and Clevers, H. (2012). Lineage tracing reveals Lgr5+ stem cell activity in mouse intestinal adenomas. *Science* *337*, 730–735.
- Schwitalla, S., Fingerle, A.A., Cammareri, P., Nebelsiek, T., Göktna, S.I., Ziegler, P.K., Canli, O., Heijmans, J., Huels, D.J., Moreaux, G., et al. (2013). Intestinal tumorigenesis initiated by dedifferentiation and acquisition of stem-cell-like properties. *Cell* *152*, 25–38.
- Steinhardt, A.A., Gayyed, M.F., Klein, A.P., Dong, J., Maitra, A., Pan, D., Montgomery, E.A., and Anders, R.A. (2008). Expression of Yes-associated protein in common solid tumors. *Hum. Pathol.* *39*, 1582–1589.
- Tolwinski, N.S., Wehrli, M., Rives, A., Erdeniz, N., DiNardo, S., and Wieschaus, E. (2003). Wg/Wnt signal can be transmitted through arrow/LRP5,6 and Axin independently of Zw3/Gsk3 $\beta$  activity. *Dev. Cell* *4*, 407–418.
- Touil, Y., Igoudjil, W., Corvaisier, M., Dessein, A.F., Vandomme, J., Monté, D., Stechly, L., Skrypek, N., Langlois, C., Grard, G., et al. (2014). Colon cancer cells escape 5FU chemotherapy-induced cell death by entering stemness and quiescence associated with the c-Yes/YAP axis. *Clin. Cancer Res.* *20*, 837–846.
- Vermeulen, L., and Snippert, H.J. (2014). Stem cell dynamics in homeostasis and cancer of the intestine. *Nat. Rev. Cancer* *14*, 468–480.
- Wang, L., Shi, S., Guo, Z., Zhang, X., Han, S., Yang, A., Wen, W., and Zhu, Q. (2013). Overexpression of YAP and TAZ is an independent predictor of prognosis in colorectal cancer and related to the proliferation and metastasis of colon cancer cells. *PLoS ONE* *8*, e65539.
- Wood, L.D., Parsons, D.W., Jones, S., Lin, J., Sjöblom, T., Leary, R.J., Shen, D., Boca, S.M., Barber, T., Ptak, J., et al. (2007). The genomic landscapes of human breast and colorectal cancers. *Science* *318*, 1108–1113.
- Zhou, D., Zhang, Y., Wu, H., Barry, E., Yin, Y., Lawrence, E., Dawson, D., Willis, J.E., Markowitz, S.D., Camargo, F.D., and Avruch, J. (2011). Mst1 and Mst2 protein kinases restrain intestinal stem cell proliferation and colonic tumorigenesis by inhibition of Yes-associated protein (Yap) overabundance. *Proc. Natl. Acad. Sci. USA* *108*, E1312–E1320.